Available online at www.sciencedirect.com
ScienceDirect
Cement and Concrete Research 38 (2008) 275–289
Cement and Concrete Research

Refinements to colloid model of C-S-H in cement: CM-II

Hamlin M. Jennings

Civil and Environmental Engineering, Materials Science and Engineering, Northwestern University, Evanston Il 60091, United States

Received 1 May 2007; accepted 29 October 2007

Abstract

This paper describes a second generation model for the nanostructure of C-S-H based on the interpretation of water sorption isotherms. The cornerstone of the model is a description of the globules (used here to mean small brick like particles), which consist of solid C-S-H and internal water, and the distribution of water in the small pores between them. Microstructural changes that occur during drying and account for both reversible and irreversible shrinkage are described. Since globules are particles, the properties of C-S-H gel are best understood through application of the emerging granular mechanics. This new model should help to establish quantitative relationships between the nanostructure and bulk properties.

Keywords: Calcium–Silicate–Hydrate (C-S-H); Microstructure; Physical properties; Characterization; Aging

1. Introduction: background of model

Some, if not most, of the mechanisms that govern the extremely complex engineering properties of concrete occur at the nanometer level. Any comprehensive model of the nanostructure should embody features that can provide a basis for establishing relationships between structure and properties. Progress has been made, but many challenges remain. For example, in a series of papers [1–4], a model has been described that rationalizes a range of experimental values for density and surface area measured for different samples, using several techniques. This nanostructure model is referred to here as the "Colloid Model I" or CM-I.

The basic units of this model are globules of C-S-H (the name globule will continue to be used although it is acknowledged that they are not spherical and they have an internal sheet like structure, perhaps layered bricks should be used but here, for continuity with previous publications, globules is used), clusters of which pack together in two packing densities, known as high density HD C-S-H, and low density LD C-S-H. The model treats C-S-H as a gelled colloid [4] or a granular material, a concept that was first indicated by observations of very large local deformations on drying, in excess of 20% [5], far greater than is possible for continuous porous materials. C-S-H behaves more like a layered clay or a granular material than it does a porous continuous material. Moreover, many other similarities exist between C-S-H and colloids [6,7]. The use of this particle packing model, CM-I, has provided a basis for modeling the modulus and hardness of C-S-H as measured directly by nanoindentation [8–11], and has facilitated multiscale procedures to accurately predict bulk modulus.

CM-I does not, however, address the properties of drying shrinkage or creep under load. Since the irreversible components of shrinkage and creep must involve changes in the structure, or rearrangement of the globules, the packing must change without concurrent changes in modulus [11]. The model gives no indication of how tightly water is bound, or equivalently, how the structure changes as water leaves and reenters the smallest pores. Describing these processes represents a significant challenge, and the purpose of this paper is to critically reexamine model CM-I, published in 2000 [1], and to suggest a number of refinements. This paper focuses on the water in the smallest gel pores and attempts to quantitatively model data in the literature, some of which has been controversial for over 40 years. Because this model represents a significant extension of CM-I it is referred to here as CM-II.

Any given experiment generally measures one particular property, such as the quantity of chemically combined water, surface area, density, length change on drying, etc. CM-II (1)

E-mail address: h-jennings@northwestern.edu.

0008-8846/$ - see front matter © 2007 Elsevier Ltd. All rights reserved.
doi:10.1016/j.cemconres.2007.10.006

places emphasis on the interpretation of sorption isotherms, particularly for water, which have caused much discussion over the years, and (2) relates this interpretation to a number of other data. It starts with the smallest scale, about 1 nm, and works up to about 100 nm.

CM-II is, in part, a model of the state of water in the finest gel pores from the perspective of thermodynamic equilibrium, although, strictly speaking, a true equilibrium is not achieved, only a metastable state. Water comes and goes from C-S-H very slowly, although it has been noted that some extrapolation may speed the process [12]. Almost all of the experimental results presented here are from experiments performed over long periods of time, usually several months. Water that enters or leaves a pore at a particular relative pressure[1] must represent water with well-defined energy. Energy of evaporation is a function of the radius of a meniscus at higher pressures and of the interaction energy between water and the surface at lower pressures. C-S-H contains evaporable water in two physical locations 1) in pores, defined as having a free surface when empty, and 2) interlayer space, defined as space with surfaces that collapse when water is removed, allowing opposing surfaces to come in contact.

This paper first discusses the characteristics of C-S-H globules by providing greater detail concerning their size, shape and internal structure than is afforded by CM-I. Next, the packing of the globules and the characteristics of the water contained in the small pores between globules is discussed. CM-II focuses on Low Density C-S-H (LD C-S-H) because, by virtue of its more open structure, it changes the most during drying, is the deforming phase during creep, and has a structure that has been studied by techniques such as small angle neutron scattering and nitrogen adsorption (in the dry state).

2. Refinements to the description of the globule in LD C-S-H

2.1. Structure of the globules

In CM-I the internal structure of the globules was described [1] as tightly packed spheres called “basic units.” These units were further described as tiny, layered C-S-H particles, but this was stated with little emphasis and without exploring the possible relationships of this structure to the properties of the material. Since this picture is not sufficiently descriptive, and needed to be altered, the model presented here, CM-II, was developed using iterative examination of several types of data, and it is convenient to start at the nanometer scale. Of particular importance here are the results from small angle neutron scattering (SANS) that have been interpreted [13,14] as scattering from particles, called globules, not the same as the basic unit in CM-I, but with well-defined size, surface area, and packing arrangement. This section discusses the structure of the globules.

2.1.1. Density and surface area, of saturated globules

Recently, neutron and X-ray scattering techniques have been used to determine with great accuracy [15] the density and water content of the saturated globules. The density is 2.604 Mg/m^3 and the chemical formula is $C_{1.7}SH_{1.8}$. These values include all water, evaporable and non-evaporable, within the saturated C-S-H particles, but do not include any adsorbed water on the surface or any other water outside of the particles. The value for the density is accurate to four significant figures. Other values used in CM-II, such as those included in Table 1, rely on data that vary slightly in the literature and are therefore much less accurate. However, even with some uncertainty, the broad basis for CM-II is established.

As discussed in CM-I, the literature is full of seemingly inconsistent values for the specific surface area of C-S-H, an observation that was resolved by proposing two densities for packing C-S-H globules, each with a well-defined surface area and internal porosity as measured by a particular technique. Different values are associated with different proportions of these two packing densities.

The size of the globules as determined from SANS experiments is about 4.2 nm across. Based on geometry, assuming spherical particles and density described above, the specific surface area would be 550 m^2/g, and, if only C-S-H that scatters neutrons is present in the sample volume, then the measured surface area should be 1200 m^2/cm^3 [16]. However, since only the LD C-S-H scatters neutrons, which is only about 60% of the C-S-H in a paste with water/cement of 0.5, the measured value should be about 750 m^2/cm^3. Further, by taking into account pores and other non-scattering phases present in paste, the computed value of the surface area is reduced to about 200 m^2/cm^3 of paste (based on size of the particles). This value converts to about 120 m^2/g of paste, based on size and density of globules. The surface area is also measured directly by SANS using the Porod scattering region to give a surface area of about 125 m^2/cm^3 [16], which converts to approximately 70 m^2/g for d-dried paste[2]. The discrepancy between the measured 70 m^2/g and the computed 120 m^2/g may be explained by noting that the regions where two particles are close to each other do not provide the two phase interface that can scatter neutrons and, therefore, do not contribute to the Porod scattering.

An alternate explanation (although in many ways identical if the close surfaces are arranged in an ordered pattern) is that the surface area per unit mass of a globule is smaller than that of a 4.2 nm diameter sphere. In other words, if the particles are actually larger in one or two dimensions, the surface area and the mass are increased such that the surface to volume ratio is reduced. For example, an ellipsoid with a small dimension of 4.2 nm could have the mass of two 4.2 nm spheres but have less than twice the surface area, which reduces the surface area per mass. This possibility is attractive because it brings the shape closer to that seen by various microscopic techniques [17–19]. A number of shapes can bring these conflicting conclusions into

[1] Relative pressure is defined here as P/P_0 where P_0 is the vapor pressure of the gas, e.g. in equilibrium with its liquid (sometimes, as with nitrogen, at low temperature) and P is the ambient pressure. This quantity may be expressed as a percentage.

[2] 5×10^{-4} Torr, an environment of dry ice at −79 °C under vacuum.

Table 1
Density and H (water) content under various conditions

Density Mg/m^3 (length scale from center of floc)	Packing density	Pore % of volume of globule	Evaporable water (M)	Total water (M)	Logic and assumptions for model values Given value(s) from literature * Computed value(s) #	Measured value of M [Ref.] comparable to computed #
2.85* [25]		–	–	1.3#	Density of d-dried measured with water. This density is achieved by removing 0.5H	1.3–1.5 1.2 [47]
2.604* (2 nm)		9 saturated inside	0.504 total evaporable	1.8*	Globule-saturated-values from Ref. [15]	
2.25		20#	–	1.3	Globule empty of evaporable water — calculation based volume emptied by water — both interlayer and IGP space empty — 0.5 M removed — *constant volume*	18% CM-I
2.44			0.25 in interlayer	1.55#	Globule with 0.25 M H removed – *constant volume* – represents IGP empty and interlayer full (interlayer water is highly restricted and to neutrons looks like chemically combined)	Not physical for drying but captures all immobile water — 1.6 [50]
2.7			0.25 in IGP	1.55	Difference between desorption and adsorption at 11% rh=0.25 mol — this is water that does not reenter globule. From saturated globule interlayer is removed and IGP remain full. No monolayer on outer surface. Density computed by simply adding 0.25 H to d-dry or removing 0.25 H moles out of globule and contracting the globule. Volume contracted 4%.	
2.47				2.1#	Saturated globule plus monolayer at 11% rh (.25 M on surface of globule) or 8% water on d-dry	2.1 [41] Compare mole to 2.1 Hanson
2.58			0.5 #	1.85	Dried globule plus monolayer (0.25 M) 11% rh on globule adsorb (interlayer space empty but IGP full with 0.25 M). This is equivalent to 5.25 wt.% water added to d-dry (B)	0.55 [30–32]
2.31 (4 nm)	0.81	19 Outside globule Below is % of total volume	0.9	2.7#	Constrained H-contained in IGP and small gel pores	2.7 CM-II fits data of [50]
2.20 (5 nm)	0.75	25	1.34	3.14	These values are model fit and can vary	
2.12 (8 nm)	0.70	30	1.74	3.53#	These values are model fit and can vary Packing density=0.70	Compare to 4 M [41] values vary with age [47]
2.03	0.64			4	Packing density=0.65	
1.2					Single globule floc at greater scale	
1.83	0.59			5	Include the LGP	

* indicates values from the literature and # indicates computed values for CMII.

line. Thus this argument can be extended to small plates of 4.2 nm thickness and the computed surface can be reduced to 110 m^2/g. It is important that the characteristic length of 4.2 nm be oriented randomly to maintain consistency with SANS results. Small platelets would be consistent with the layered atomic structure of C-S-H. Fig. 1 shows the side view of the new particle. Another advantage of modeling C-S-H particles as elongated is the inclusion of another degree of freedom (rotation) in modeling mechanical properties, and this possibility should be more fully explored in the future.

2.1.2. Density and water content

Because the density of d-dried C-S-H, shown in Table 1, is higher than the density of the saturated globules, they must contain evaporable water. The description of how this water is contained within the particle is shown schematically in Fig. 1. Ample evidence suggests that C-S-H is, in some respects, similar to tobermorite and jennite [20], and that C-S-H has a layered structure, albeit highly disordered. In one version, these imperfect layers, with relatively large in-plane dimensions, entrap tiny gel pores [21]. In the CM-II model, these pores within the globule will be referred to as intraglobular pores (IGP), which, although they are small, are of some importance. In addition, there are gel pores that are interglobular pores between the particles. In many ways the concept of two types of small gel pores is similar to a proposed [22] variation of the Feldman Sereda model.

This is our starting point, but, as stated, consistency of the model with other data is important. To examine this, the published values of water sorption isotherms have been converted to moles of water relative to moles of C-S-H. The 1.8 M content of water in C-S-H globule includes evaporable and non-evaporable water inside the particle, but does not include any adsorbed or gel pore water. From this, either the density or water content can easily be computed if the other quantity is known and if evaporable water is assumed to have a density of 1 Mg/m^3. It will be shown that although water with much higher density (1.2–2 g/cc) has been suggested [23,24] to explain certain data, this unlikely assumption (only small increases in density are possible) is not necessary. The data used

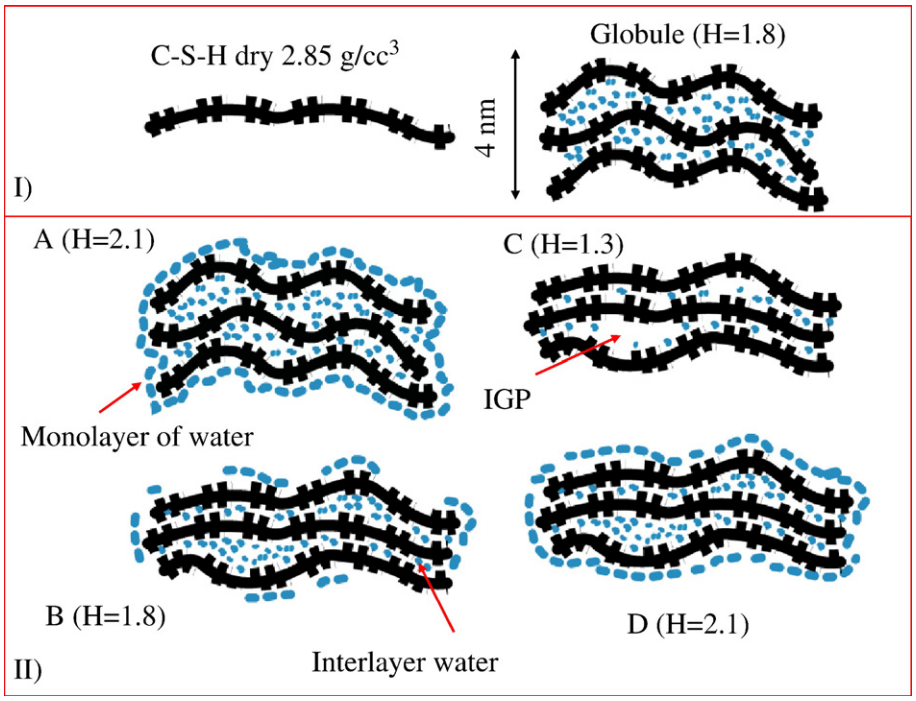

Fig. 1. A schematic of a globule with water contents representing various states achieved during drying from 11% rh and rewetting to various relative humidities and then returning to 11% rh. I) Single sheet of C-S-H with all evaporable water removed, and a saturated globule without water adsorbed on the surface. II) A) Fully saturated globule with monolayer on the surface and both interlayer and IGP full representing 11% rh. B) Partially dried with much of the interlayer water and monolayer removed. Volume of globule plus monolayer is reduced and density is increased from that of saturated globule. C) All evaporable water removed to represent the d-dried state. The IGP are empty leaving internal void and reducing density. D) On rewetting water is returned to the IGP and a monolayer is present. The full IGP increases density.

to hypothesize a very high density will be explained according to CM-II later. All experimental densities for C-S-H are corrected for the presence of CH, as suggested by Taylor [20], and are, therefore, slightly higher than uncorrected values.

The density for d-dried C-S-H [25,20] (corrected for CH) has been measured by water pycnometry to be 2.85 Mg/m^3 [25]. This measured value for the density of the solid without the water is computed theoretically by removing 0.51 mol of water from both intraglobular pores and interlayer space. The water content of d-dried C-S-H is therefore 1.3 mol, within the range that has been measured for C-S-H [25]. Slightly more water can be removed if the sample is oven dried, perhaps bringing the content to 1.2 mol as has sometimes been reported [20].

2.1.3. Sorption isotherms

The development of CM-II has relied heavily on data from sorption isotherms. Over the years, much effort, both theoretical and experimental, has been directed toward interpreting gas sorption isotherms. Different gasses lead to different values for the specific surface area, and experimental results using water vapor produce a very confusing isotherm. The surface area has often been evaluated using the BET [26] method, which uses any gas that wets the solid at the temperature at which the gas condenses onto the surface. It is presumed that, starting with a clean surface, the first layer of molecules adsorbs with an (higher) interaction energy while the second and subsequent layers adsorb with another (lower) interaction energy and that this water is liquid like. Ideally, when weight gain is plotted against the relative pressure of the gas, the slope has one value while the monolayer forms and another value during the formation of subsequent layers. The amount of gas adsorbed when a complete monolayer has formed gives the surface area. Two of the most commonly used gasses for this procedure are nitrogen and water vapor.

2.1.3.1. Nitrogen. Nitrogen has been used extensively to measure the surface area of cement paste and the isotherm is fairly easy to interpret (see for example Refs. [27,28]). The shape of the typical nitrogen isotherm is shown in Fig. 2. There is no low-pressure hysteresis (below a relative pressure of 50% relative to saturation), and at higher pressures the hysteresis is a consequence of capillary condensation, the capillaries rupturing as nitrogen is removed and not reformed during adsorption until higher pressures.

Although the isotherm for any one sample is well behaved, there are large differences from sample to sample, and the values obtained for surface area vary greatly when portions of a given sample has been dried using different techniques. Furthermore all of the values for surface area derived from nitrogen sorption do not come even close to agreeing with values obtained by adsorption of other gases, in particular water vapor, and the values depend on the water/cement ratio of the sample and other variables. Indeed, almost every gas that has been used for BET experiments (see for example Ref. [29]) produces a different value for surface area. These, and other observations, were taken into account in CM-I, by proposing

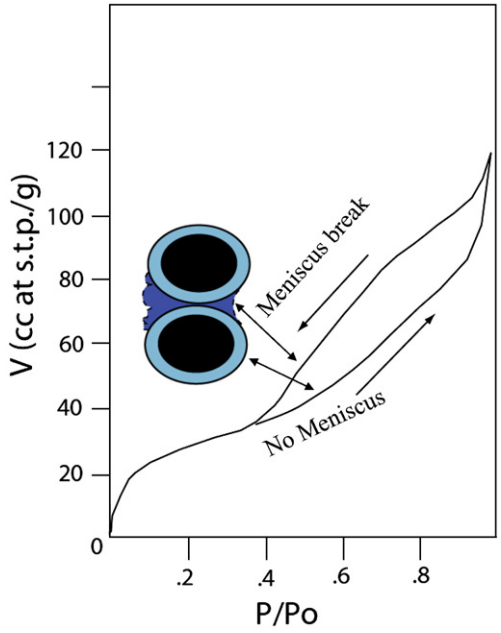

Fig. 2. Nitrogen isotherm for cement paste. The hysteresis is due to stable meniscus during desorption which does not reform during adsorption until high partial pressures are achieved. Data from different researchers and data using different drying techniques vary somewhat.

that the globules pack into two densities, LD (low density) and HD (high density), and the different surface areas depend on the relative proportions of the two, controlled by, for example water/cement ratio. Nitrogen penetrates only the LD structure, and, therefore, the surface area depends on the amount of LD formed in a particular sample. Since LD forms mostly during the early stages of the hydration reaction, the nitrogen surface area, for gently dried samples, is almost fully developed during the early reaction [1]. The highest measured values of surface area, for very gently dried samples, are very close to that obtained from SANS. However, some lower and higher values have been reported and these will be discussed after the CM-II model is more fully presented.

CM-I provides no detailed insight about changes in the nanostructure due to heat, age of the sample, relative humidity history, or the closely related creep under load, although some hypotheses have been proposed [3,11]. One of the implications of CM-I is that nitrogen surface area highlights with some success an important variation in microstructure that is associated with properties, but CM-I leaves exact relationships with creep and shrinkage far from complete. Part of the objective of CM-II is to describe the influence of heat, relative humidity, and age on the nanostructure.

2.1.3.2. Water vapor. Water sorption isotherms have also been studied extensively and comparison of the results from different researchers shows that they are reproducible. They result in a much higher value for surface area than do nitrogen isotherms, and the value is relatively constant from sample to sample, including samples of different age, curing temperature, and relative humidity history. These results are obtained from the adsorption branch of the isotherm after conditioning the sample to a specific moisture content (rate of drying seems unimportant), usually by drying to the so-called d-dry state [20,24]. Under the assumption that C-S-H is well defined as a material, it should have a well-defined specific surface area. Fig. 3 is a typical water isotherm using typical (different investigators are in close agreement) data by Powers and Brownyard [30], Brunauer [31], and Feldman [32].

The major problem in interpreting the water isotherm is the large hysteresis observed at pressures (P/P_0) less than 50%, which has been the subject of much debate [33–37]. Furthermore, the isotherms change significantly between first drying and subsequent drying. After d-drying, the adsorption isotherm of the sample becomes linear at around 11% relative humidity (this is sometimes reported to be as much as 20%, which changes the amount of adsorbed water only slightly and does not affect the main arguments presented here), and this is interpreted as the point at which a monolayer of water is complete. Apparently, the surface area is about 300 m^2/g of saturated C-S-H [1].

Various qualitative explanations have been suggested to explain the difference between nitrogen and water sorption [24,33]. On the one hand, it is argued that water penetrates the smallest pores giving the correct values [38,39], while nitrogen does not penetrate the "ink bottle" entrances to these pores. On the other hand, some investigators [40] suggest that water enters the interlayer spaces, which, because they collapse and do not create free surfaces on drying, should not be considered pore space, and that therefore the water results give a calculated surface area that is much too high. The difference between these interpretations is not trivial, since the role of water in these smallest spaces depends on whether it is adsorbed on a free surface or resides within the structure, and there has to date been no definitive resolution of this question.

The desorption branch of the water isotherm (for both first and subsequent dryings) has not been analyzed as extensively as the adsorption branch, mostly because it is difficult to interpret with only a small linear region and a complex hysteresis, but it is proposed here that it provides a great deal of useful information. All of the data discussed here were obtained from experiments in which equilibrium or near equilibrium conditions were achieved: samples were conditioned for long periods of time, usually many months, which means that explanations for water content should be based on the assumption of thermodynamic equilibrium, and not rely on kinetic arguments.

Data for density and water content of C-S-H have been gathered from experiments where the sample is either saturated, d-dried, or equilibrated at 11% relative humidity. The major observations are included in Table 1. Water content is expressed in terms of moles of water in the C-S-H (requiring the conversion of most data in the literature), and includes both chemically combined and evaporable water. Thus, the formula for C-S-H has been determined as $C_{1.7}SH_x$ where x is the number of moles of water. As described above, based on density measurements, the water content of d-dried C-S-H was computed to be 1.3 mol. All water in excess of this value is considered evaporable.

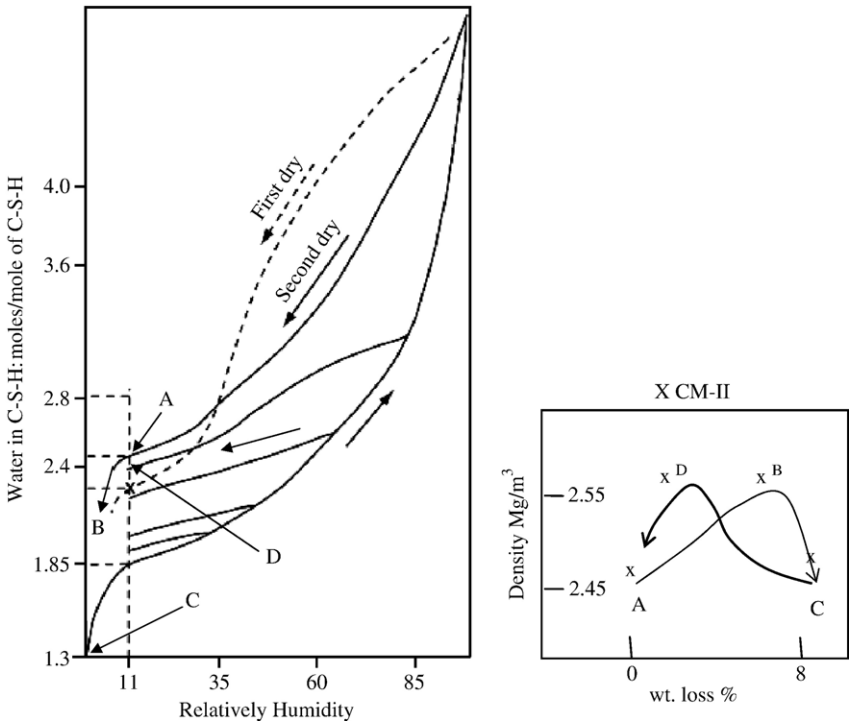

Fig. 3. Water isotherm using data adapted from two publications, which captures the features of several publications referred to in the text. The first drying is from Powers and Brownyard [30] and the second drying and rewetting is from Feldman [32], both for samples with water/cement=0.5. All data have been converted to moles of water in C-S-H, including bound water and water that is removed and returns on drying and rewetting. Both references explicitly note that the water content at 11% rh was greater on second drying than on the first, as is shown.

Interestingly, if the water content of a saturated globule with a monolayer of water on the surface is taken to be 2.1 mol [41], and if the content within the globule is 1.8 mol, then the surface area can be estimated. Assuming the difference between $x=2.1$ and $x=1.8$ is a monolayer of water:

$$\frac{0.3 \text{ mol water}}{1 \text{ mol CSH}} \times \frac{1 \text{ mol CSH}}{188 \text{ g}} \times \frac{6.02 \times 10^{23} \text{ water molecules}}{1 \text{ mol water}} \times \frac{11.4 \text{ A}^2}{1 \text{ water molecule}} \times \frac{(1 \text{ m})^2}{\left(1 \times 10^{10} \text{A}\right)^2} \times \frac{2.6 \text{ g CSH}}{1 \text{ cm}^3 \text{ CSH}} \times \frac{0.4 \text{ cm}^3 \text{ CSH}}{1 \text{ cm}^3 \text{ paste}} = 114 \text{ m}^2\text{m}^{-3}$$

The last term before the equal sign represents the volume fraction of SANS C-S-H in a paste [42]. The result is very close to the SANS surface area for a mature cement paste.

2.2. Model for water content of the globules

The next step is to model the evaporable water within the globule. Here, in contrast to previous models, CM-II includes two locations, the interlayer space and the intraglobular pore (IGP), each of which contains water with its own binding energy. The problem is to model water in the interlayer space as opposed to that in the IGP, and to justify the need for the two types of water in order to interpret literature data. The entire water isotherm, including the low-pressure hysteresis, requires a model that takes into account the location of water within the saturated globule.

The removal of water from the interlayer space causes the globules to collapse, and the removal of water from the IGP empties "pores" with no change in volume of globules. As will be discussed, removal of adsorbed and/or interlayer water increases the density of the globules and removal of water from IGP decreases the density. Removal and resorption of water is a very slow process and one possibility is that structural changes associated with the redistribution of water occur during this process. In other words the sheets of C-S-H change shape and orientation with respect to nearest neighbors. This structural change may be the source of an activation barrier to the motion of water in and out of the interlayer space, or a change in energy with associated stress. While it is not possible from the information presently in the literature to state exactly which category of water leaves or reenters the globules first on drying or rewetting, density measurements narrow the possibilities, and the following paragraphs model the data well.

2.2.1. 0–11% relative humidity

The desorption isotherm is nearly linear over a small range just above 11% rh, a point where a monolayer has formed on the globule. Thus both the adsorption and desorption isotherms provide information about water content of the globules with a monolayer on their surface. However, CM-II models the linear portion of the adsorption isotherm as water forming both multiple layers on the surface and entering the globule. Since the slope of the isotherm is constant, the energy of both these

populations of water is the same, and the most likely location for the internal water is multiple layers in the IGP, as will be discussed below.

The difference between adsorption and desorption is consistently about 0.25–0.30 mol water ($C_{1.7}SH_n$ where n is moles of water), depending on how much the sample is ultimately dried. This model uses the value of 0.25 mol (converted from weight percent) based on the careful experiments of Brunauer [31], which are in agreement with Feldman's results. However, it should be noted that adding (or subtracting) a little evaporable water does not change the model presented here, it simply means that less water is in the dried state of C-S-H (perhaps oven dried), and this water can be simply added to the water removed when dried below 11% rh.

In CM-II, 0.25 mol of the water present on desorption from 11% does not reenter the structure upon resorption to 11% rh. This value is greater on second drying (0.55 mol), which will be discussed later. Desorption from 11% rh increases density [32], modeled here by water being removed from the surface and from the interlayer space, both of which tend to increase density in the same way (both volume and mass change the same amount when water is removed from either location). Finally removal of IGP water decreases the density of the C-S-H. The fact that resorption to 11% rh does not change density of C-S-H means that water both enters the IGP (effect of increasing density) as well as adsorbs on the surface (effect of decreasing density). Thus water is removed from but does not reenter the interlayer space during desorption and adsorption below 11% rh. This irreversibility could result from the deformation of the layers during drying that does not recover until higher humidities. In other words, water only reenters the interlayer space when multiple layers of water on the surface reduce the surface energy and allow the structure to relax. Alternatively, this might be thought of as resulting from a positive pressure due to strong adsorption forces developing as water enters the intraparticle pores, which has the effect of opening the interlayer space. Perhaps this is similar to deformation observed in zeolites due to adsorption [43]. One way or other this may be associated with the interpretation [44] that an energy difference is responsible for the observed hysteresis. Again, detailed molecular dynamic modeling may elucidate the details of this adsorption/desorption problem.

When a d-dried sample is equilibrated to 11% rh, about 0.55 mol of water are added (using data from Feldman, Brunauer as per Fig. 3). The question is how much is on the surface and how much is within the C-S-H globules. Although this question has been answered above, it is useful to approach the problem from a slightly different angle, which can also demonstrate the robustness of the model. The hysteresis observed at 11% rh is interpreted here as resulting from the globules having a monolayer on the surface; the interlayer space is empty; and the IGP have an internally adsorbed layer making them partially full. At higher relative humidities these interior spaces become more filled. Thus during adsorption, of the 0.55 mol added to C-S-H, 0.3 mol form the outer monolayer, and 0.25 mol enter the structure with the same thermodynamics as water adsorbing on the outer surface, leaving 0.25 mol of water that was irreversibly removed and only reenters at much higher rh's. (During the first drying, the structure contained 2.1 mol at 11% rh, which is 0.55 plus 0.25 plus 1.3 mol. This observation, namely that on adsorption to 11% rh some of the water reenters the globules and some does not, and the assumption that the surface area of the globules does not change as a result of drying, forces the concept of two types of space within the globules, one into which water can reversibly reenter and one which water cannot reversibly reenter.

While CM-II assigns values for the amount of water in IGP and interlayer space, there are also implications to the surface area. Since adsorption above 11% rh is linear, the water is thermodynamically similar to multilayer adsorption. Since the value of external surface area is about 1/2 that implied by water adsorption, almost 1/2 of the surface area must be internal. The surface of the IGP must therefore adsorb water at pressures below 11% rh.

If the absolute water content of the globules were unknown, the CM-II would predict the same result using the surface area data from Porod scattering or nitrogen sorption and subtracting the appropriate amount of water in the monolayer to give the internal water content, but the necessary values for this calculation are somewhat scattered and are known with poor precision. Thus, central to the concept of CM-II, are globules with water in three locations: (1) adsorbed on the outer surface as a monolayer, (2) adsorbed within the particle, in the IGP, and (3) located in the interlayer space, capable of causing swelling and internal strains. The idea that water only very slowly leaves and reenters globules, and that this process may be associated with strain, may be important to understanding reversible creep and viscous deformation. Additionally, at higher relative humidities, water exists between the globules.

2.2.1.1. Feldman's helium experiments. The water content of the globules, as defined above by CM-II, can be tested in some detail. In the early 1970s Feldman [32] published the results of complex experiments that determined the density of C-S-H with different water contents, all at or below 11% rh. When water was removed, the sample was equilibrated to an rh less than 11%. When water was added to the dried sample, conditioning occurred at higher rh's and then the sample was returned to 11% rh. As the samples were exposed to higher rh's more water reentered the structure, much of which remained after desorption back to 11%. The 11% rh is associated with the point at which a monolayer is present, but in addition, water also enters the structure as the rh is increased. These experiments demonstrate that the hysteresis is caused by water leaving the structure at low rh and not reentering the structure until higher rh's.

Feldman measured two densities, one using the volume that was quickly occupied by helium and the other when helium was allowed more time (40 h) to penetrate almost all of the pore space. The interpretation presented here, different from Feldman's, is that the latter represents all of the space outside of the globules. Predictions of CM-II must now be tested against Feldman's data. To do this in the model, water is added to and subtracted from the globule in the three locations. (1) On the surface to form a monolayer where it increases the volume of

the globule as well as the water content. This condition exists at 11% rh; (2) Within the IGP where it adds to the water content without changing the volume of the globule; (3) In the interlayer space where it changes both the volume of the globules and the water content. The numerical values for the densities of all permutations of these conditions are included in Table 2.

Interpretation of Feldman's experiments is as follows: Before drying below 11% rh, the globules are covered with a monolayer. Nevertheless, this model suggests that water is first removed from the exterior surface and then from the interlayer space. Water in the interlayer space may have a relatively high free energy because a free surface is not created with the removal of this water. This is perhaps surprising but may also be due to the role played by cations in the interlayer and/or in IGP. These ions have been shown to strongly influence how water enters and leaves montmorillonite [45]. The removal of interlayer water and surface water both have the effect of increasing the measured density. However, water in the interlayer space is the source of the hysteresis as has been postulated in the past (see for example Refs. [20,24,46]). What is different here is that the interlayer water leaves the globules before the water in the IGP does. The IGP water leaves at the lowest rh's with the result that the density is reduced.

At 11% rh a monolayer is formed on the IGP and on the outer surface. When more water is added in an amount roughly up to 0.55 mol, it fills the IGP and also adsorbs on the outer surface. These combined effects increase the density of the globules to about 2.6 Mg/m^3. Also, since only about half the water, namely the outside surface water, changes the measured volume, and the other half enters the IGP, the implied density of water is nearly 2 Mg/m^3, a value near that measured by Feldman and not easily explained until examined in the light of CM-II. Finally, at higher rh's, as stated in Feldman's original arguments, water increasingly enters the interlayer spaces.

As shown in Fig. 3, C-S-H contains less water at 11% rh on the first desorption than on the second and subsequent (not shown) desorption isotherms. This is interpreted here as the result of the creation of interlayer space by the approach and reorientation of neighboring globules during the first drying, which causes a larger hysteresis.

2.2.1.2. 11–40% relative pressure. Approximately another 0.25 mol of water enters the gel pores when the pressure is increased from 11 to 45% relative humidity or, similarly, this amount of water is lost during drying. As this interlayer space is filled, the globules expand, resulting in an apparent density of water of about 1.2 Mg/m^3, as measured by Feldman. The expansion of the globule reduces its density. The above analysis of Feldman's experiments, using CM-II, is the first quantitative interpretation of his results, and the agreement between the data and the model is good. It also resolves recent statements [47] that the first adsorbed water is "compressed" by about 10%, by noting that some of the first adsorbed water enters the globules.

Within the limits of these pressures, the isotherms exhibit nearly a constant difference between adsorption and desorption, equal to about 0.25 mol. Apparently the irreversible water is tied into the structure until pressures below 11%, at which point it is removed, or until pressures higher than 40% rh, at which it reenters the structure.

2.2.1.3. 40–60% relative pressure and above. Another 0.25 mol of water are gained between 40–60% rh. On desorption, capillary water (or water with a meniscus) is stable within this range, but during adsorption, it does not reform, and this increases the difference between adsorption and desorption. It is seen as a bump on the desorption curve when the meniscus becomes unstable, at which point all of the water evaporates until a layer of only several molecules remains.

Powers [38] defined capillary water as water that is not thermodynamically influenced by the surface of C-S-H, and therefore must be located at least two water layers away from the surface. The capillary water on desorption above 40% rh is therefore not gel pore water even though the meniscus may be within the bounds of the volume of C-S-H. This has implications when comparing C-S-H gel to other gels. Gel pores have also been defined as pores within the C-S-H and therefore this population increases with percent reaction. Finally, gel pores may be defined as pores that are not emptied at about 85% rh [3], which is the definition adopted here. These different definitions of gel pores has lead to confusion, which will be discussed in future publications, here gel pores mean the pores that are an intrinsic part of C-S-H, with diameters of less than about 20 or so nm's.

The Roper curve for shrinkage vs. weight loss shows a marked decline in shrinkage at about 35–40% rh [48,11] as does direct measurement of shrinkage using an electron microscope

Table 2
Data and model for comparison to Feldman's experiments (corrected for CH)

CM-II Density Mg/m^3	Moisture condition	Experimental Density by He corrected for CH [20,76]	Comment	Position in Fig. 3
2.47	11% initial dry	2.45	Globule plus monolayer at 11% rh monolayer (0.275 M on surface of globule)	A
2.60	Partial dry to d-dry	2.55	Monolayer without interlayer or interlayer without monolayer or any combination – holding total volume and total mass constant – IGP full	B
2.25 – 2.53	d-dry	2.45	Globule empty, no monolayer – density depends on degree of interlayer collapse – highest density completely collapsed – IGP empty – complete collapse is not possible so predicted density between values	C
2.60	11% adsorb from 47% rh	2.40 – 2.55	Globule collapsed – IGP full and monolayer: 5.25 wt.% gain from d-dry	D
2.30		2.30 – 2.36	Include empty SGP (8%) – correct for CH – short term He inflow — see text on particle packing	

[5]. This point is similar to the "critical" point observed in gels [49] when the interface between liquid and gas enters the pores between the gel particles, which results in much reduced shrinkage and sometimes even expansion. By plotting length change against weight change when a prism of C-S-H paste was dried, Roper [48] was able to clarify the different mechanisms of shrinkage. At just below 40% rh, the paste almost stops shrinking, and this has been identified as the critical point for C-S-H gel, but it should be noted that pores larger than about 2 nm radius are empty at this point. In other words, the critical point defines a point when the large gel pores (LGP) are empty, and these are pores within the volume of the gel. The LGP are thermodynamically similar to capillary pores.

An estimate of the water content on desorption at 35–40% rh is 2.65 M, close to that identified as constrained water by quasi elastic neutron scattering, (QENS) [50] and to many other physical and chemical changes seen at around 33% rh [51]. If the interlayer water is relatively immobile it is seen by QENS as chemically combined. If this is so, the 0.25 mol of interlayer water can be added to the 1.3 mol of chemically combined water to give 1.55 mol of immobile or "chemically combined" water, close to the 1.6 mol measured by QENS.

3. The relationship between the packing of globules and the properties of the C-S-H

3.1. Granular structure and properties

Both CM-I and CM-II are founded on the idea of packing particles (globules) that have surface area, internal porosity, and interlayer space. The spaces between the packed globules are referred to as small gel pores (SGP). This hierarchy of water-filled volumes, inherent in CM-I, is the only way found to date to quantitatively explain a reasonably large body of data. Thus, both CM-I and CM-II are based on the assumption, shown to be viable by the close fit between experimental data and model predictions, that C-S-H is fundamentally particulate or granular in nature, as explicitly suggested by Powers and Brownyard [30], and, more recently, by analysis of results from nanoindentation experiments [10]. Using the self-consistent scheme, in which the influence of both pores and particles are separately homogenized to a consistent property at a larger scale, predictions of the influence of packing density on modulus have been derived and compared to the more developed Mori-Tanaka homogenization process. This analysis points to the granular nature of C-S-H, with both the HD and the LD modifications composed of the same C-S-H particles with identical properties, only packed differently. Assuming this to be true, unique relationships between packing densities, the number of particle contacts, and the volume of porosity are predicted. This point will be discussed below.

Implicit in CM-II is the concept that C-S-H globules have a structure with specific internal and surface properties. This allows the apparent density to vary with relative humidity, and it allows properties to vary at the 100 nm scale, without changing the globule structure, by simply packing the globules into different arrangements. Thus, packing density of globules can change, while maintaining other properties, such as the constancy of water surface area.

3.1.1. Particle packing

The distribution of water in CM-II is highly constrained at the globular scale, with only one viable distribution of water inside and on the surface, but there is some flexibility at longer length scales. This flexibility comes in part from the granular nature of C-S-H, which is an important aspect of this section.

The LD packing pattern is fractal, and has been described in CM-I [1]. The new shape of the globules and schematics of proposed packing arrangements are shown in Figs. 1,4, and 5. A number of conflicting concepts have had to be resolved, or partly resolved, in the development of CM-II. With a fractal dimension close to 2.6 at scales between a 4 and 100 nm's, it is impossible to achieve the density implied by CM-I and observed by nanoindentation [11]: namely a packing density of 0.64, the equivalent to random jammed packed spheres, a concept that may be somewhat misleading for the packing arrangement. With the new concept of the globule shape, an explanation of this observed packing density of 0.64 no longer depends on jammed packing [52], and there is some flexibility in the arrangement of particles to accommodate deformation.

One possibility for the packing arrangement is shown in Fig. 5 where fractal regions, or globule flocs, (GF), overlap. The overlap allows the average density to increase greatly over that of a single GF. The fractal dimension for a GF is:

$$(1-p) = r^D$$

where p is the volume fraction of pores within a radius r and D is the fractal dimension. Using the densities and scales included in Table 1, a fractal dimension of 2.67 is computed, which is similar to that derived from CM-I. However, even with overlap, an average packing density of 0.64 is difficult to achieve, and certainly can not

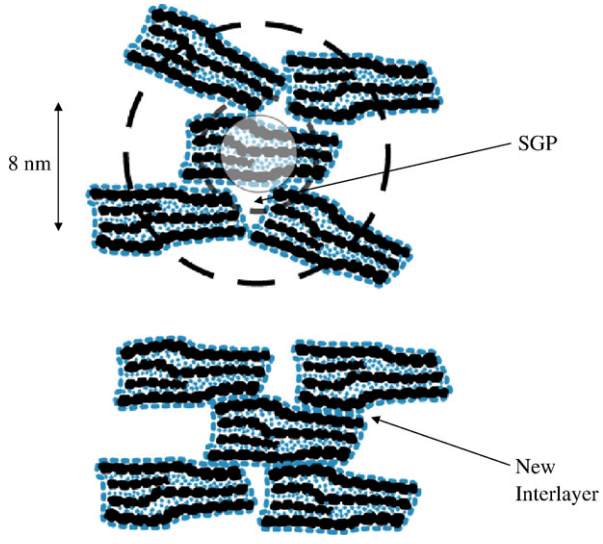

Fig. 4. Packing of globules showing small gel pores (SGP). The SGP represent an additional 12% porosity outside of the globule implying a saturated density of 2.23 Mg/m^3, in almost exact agreement with Feldman's measured density using short time He inflow.

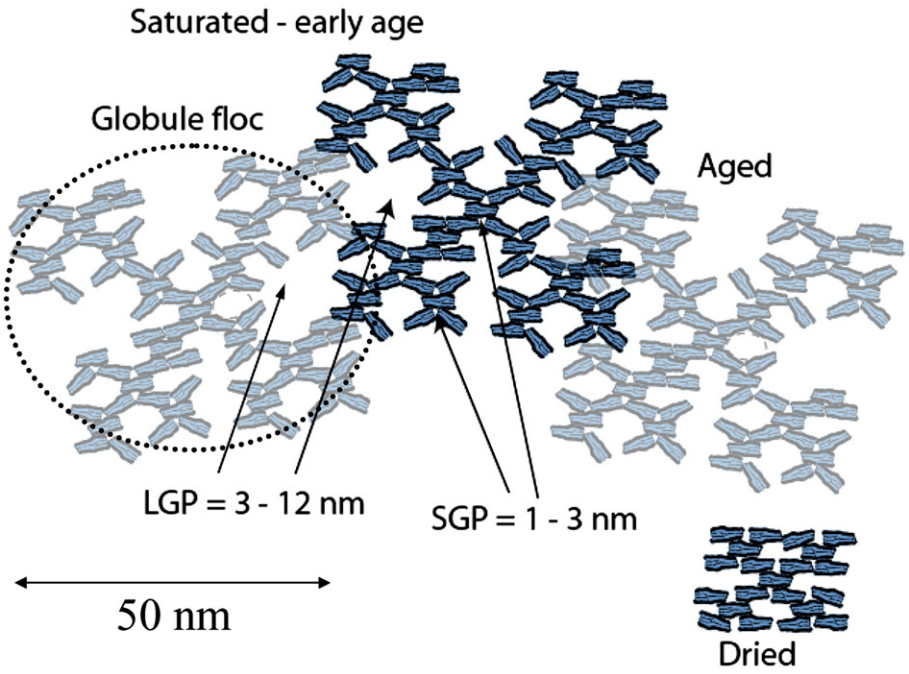

Fig. 5. The aging process schematically represented as progressing from left to right. Time, drying, temperature and probably applied stress change the structure form the more open to the tighter packed as represented on the right. During aging the large gel pores are reduced in size and volume, the globules align.

be maintained during deformation and/or shrinkage, and this problem will be discussed in the following sections by analyzing the particle packing at each of several scales.

3.1.2. The globule and its immediate neighbors — 3 nanometer scale

Fig. 5 is a schematic of a globule and its immediate neighbors. It is easy to construct arrangements having very small porosity trapped between the globules, which we will refer to as small globule pores (SGP) that are percolated to the outer regions. These pores are assigned a volume equal to 12% of the volume of a globule but are located outside of the globules or between adjacent globules, consistent with a number of experimental results. This gives 2.3 Mg/m^3 as the density of water-filled C-S-H at the scale of 3 nm, consistent with the density of a fractal structure. It also computes to the density, if these pores are empty, as measured by Feldman using results from helium inflow pycnometry experiments before the helium was allowed to flow into the smallest pores. In addition, it gives a water content equal to that of constrained water plus chemically bound water as measured by QENS [50].

An important parameter behind the development of CM-I [53] is the quantity of "nitrogen inaccessible" pore space in the LD structure, which is greater in the LD structure than in the HD structure. Using published data [53], one can compute the effective density of the LD C-S-H that includes only the volume inaccessible to nitrogen (i.e. globules plus inaccessible pores) to be 2.2 Mg/m^3, which is again very close to that computed for C-S-H plus hindered water in Table 1, both with the pore (SGP) empty. Feldman's short time (immediately after exposing the sample to 2 atm pressure) helium density is also consistent with this value [32]. This analysis implies that hindered or constrained water occupies the same volume as has been assigned as "nitrogen inaccessible." Interestingly, the 'hydraulic radius of the pore system inaccessible to nitrogen for samples older than one day tend to an average limiting value of 11.1 Å [54]. This is nearly identical to the 1.1 nm SGP.

The short time helium inflow experiments can be interpreted in some detail. Upon first drying from 11% rh, both volume and weight are reduced such that the overall density does not change much. At the 3–5 nm scale (radius) the volume is reduced by effectively packing the globules more tightly. As water is removed from the surface of the globules, they rearrange to reduce the high surface energy, thereby reducing the SGP, which are empty and can fill with Helium over time. The density of the globules increases as discussed above, so that the measured density by short term Helium inflow remains constant. The rearrangement changes some of the outer surface of globules to interlayer space, reducing the surface area, as measured by SANS by roughly 20% [55]. On rewetting, water first reenters the IGP as well as forming a monolayer on the surface, causing the density, as measured by helium inflow experiments at 11% rh, to increase. Finally, as the interlayer spaces are penetrated by the helium, the assemblies of globules expand and density is reduced. Because aligning the globules has created interlayer space, expansion continues as water enters.

3.1.2.1. 3–30 nanometer scale. At scales greater than 3 nm, CM-II has flexibility for explaining a wide range of data, and consequently the details of the model require further research. One possible fractal arrangement is shown in Fig. 4. Simply repeating the 3 nm structure preserves self-similarity. Adjacent

globule flocs overlap, entrapping pores between 3–12 nm across. It is these larger gel pores that are removed during irreversible shrinkage, which in turn, may result from the rearrangement of particles [3] and not, as proposed by the Feldman school, from sliding the layers of C-S-H within the structure. However, deformation of the globules may occur when they are under stress, and this deformation may be recoverable.

It is evident that the average packing density must be less than 0.64, the random jammed packed density [52], if the 3–12 nm pores are included in the calculation. As described above, these pores are not part of the gel porosity as defined by Powers and Brownyard, even though they are within the boundaries of the C-S-H. The large capillary pores, outside of the C-S-H, are empty at 85% rh.

Reduction in the number of pores between 3–12 nm occurs with age, heating, and drying, which all have the effect of reducing the pore content of LD C-S-H and increasing the capillary pore space. However, the mean value of modulus does not appear to change (at least on heating [11]), although the distribution around the mean does. This is not compatible with continuum mechanics and can perhaps be addressed by deeper investigation of the properties of granular materials. Experiments reported in the geotechnical literature [56] have shown that sands with non-spherical shapes can preserve a constant modulus while changing packing density and visa versa. What is probably important here is the number of nearest neighbor contacts, and future research into this should be productive. Perhaps the best way to study this problem is with advanced discrete particle models.

3.2. Implications for shrinkage and creep

Two of the most important properties of concrete are drying shrinkage and creep under load. Both of these properties have reversible and irreversible components. The mechanisms responsible for reversible shrinkage have been discussed extensively, and will be revisited in light of CM-II, but irreversible components have received little explicit discussion in the literature. For the purpose of this model it is convenient to divide the pores that exist within the gel volume into three categories. (1) The IGP has already been discussed. (2) The small gel pores (SGP) that exist outside the globules but are less than about 3 nm across. And (3) the larger gel pores (LGP), here defined as those between 3–12 nm. First irreversible and then reversible shrinkage will be discussed, followed by comments on creep.

IGP≤1 nm
SGP = 1 − 3 nm
LGP = 3 − 2 nm

The 3 nm break between SGP and LGP is somewhat arbitrary; it is chosen as roughly the size of the pores that empty when the meniscus becomes unstable, or the largest size of pores remaining full at about 40% rh.

3.2.1. Irreversible shrinkage

Theories for irreversible shrinkage are scarce, although correlations have been made between increased polymerization of silica, increased capillary porosity and total shrinkage [58]. The simplest and most obvious explanation offered by a model that considers the granular nature of C-S-H is that permanent deformation is the result of the lateral movement and/or rotation of the globules. Since the globules are not spherical, translation and rotation can reduce surface as discussed above and shown in Figs. 4 and 5.

Feldman's data, [58] along with ours [3], suggests that essentially all irreversible shrinkage is achieved by drying from 100% to 50% relative humidity. Further drying is mostly reversible, except perhaps when carried out between 11% rh and d-dry conditions. At 50% rh, the LGP are empty, suggesting that these pores must contain water to facilitate irreversible shrinkage. Also, the volume of LGP is reduced during first drying, and is not much changed during subsequent drying, and SANS data indicates that the correlation length is reduced [11]. Irreversible shrinkage is modeled here by pushing the interpenetrating globule flocs closer together, a process driven by a meniscus surrounding all of C-S-H, i.e. the meniscus is at the edge of the capillary pores, or at the edge of the LGP at rh between 85–40%. This is schematically shown in Fig. 5. Possibly some reorientation of globules also occurs. In addition to the meniscus effect, capillary tension, contributes to irreversible shrinkage, which is accompanied by very large local volume changes as has been observed in an environmental electron microscope [5]. This tighter packing of globules can also be correlated with an increased degree of polymerization of the silicates, and a somewhat reduced measured surface area. However, the mechanical properties of granular material require more study.

3.2.2. Reversible shrinkage

The mechanisms behind reversible shrinkage have been discussed [59] and broadly accepted. Shrinkage is analyzed in terms of surface tension, capillary tension and disjoining pressure. The CM-II model, however, adds other possibilities to these mechanisms. Certainly capillary tension is of central importance at relative humidities higher than 50%. Shrinkage can be analyzed [60,61] at the higher relative humidities, above 30–40%.

$$\varepsilon = \frac{\Delta V}{V} = \sigma\left[\frac{1}{3K_{\text{composite}}} + \frac{1}{3K_{\text{solid}}}\right] V[r(RH)]$$

where K is the bulk modulus of the composite or the solid (excluding the pore), V is the volume fraction of filled pores (varies from 0 to 1) of size less than r at a particular relative humidity, and ε is the strain. There is nothing in this model to change the role of capillary tension on shrinkage. At somewhere around 40% rh the LGP are empty and the meniscus becomes unstable. This is the critical point and the air water interface enters the SGP, accompanied by much reduced shrinkage or even expansion. This type of problem should be analyzed in terms of a compacting colloid.

For low relative humidities, Powers tried to analyze shrinkage in terms of surface energy of the particles. Removal of the last layer or two of water increases the surface energy of the C-S-H, as it does for any material. Noting that there are no

chemical reactions during this change, Powers determined that the heat of adsorption (heat of immersion according to Powers [38]) is close to the free energy change. Thus:

$$\Delta G = -\Delta H = a\Delta\gamma$$

and

$$\Delta\gamma = -\frac{RT}{a}\int_0^p n\frac{dP}{P}$$

where

G	free energy
H	enthalapy
a	surface area
P	pressure
γ	surface energy of solid
n	number of moles

Finally

$$\frac{\Delta l}{l} = k\Delta\gamma$$

where

$$k = \frac{a\rho}{E}$$

where

ρ	density of C-S-H
E	Young's modulus

These are the Bangham equations. The values used for a globule are E=60 GPa [62] and a=70 m^2/g. Evaluating these equations below 40% rh gives a change in length of 0.05%, far lower than the observed 0.3%. Recently, this disparity between theory and observation has been critically analyzed [63].

The volume change indicated in Table 1 resulting from removal of interlayer water gives a length change of 1.5%. Bulk measurements indicate that this volume change is too large, but it should be noted that shrinkage of 1% or more has been measured directly for small regions of C-S-H using microscopic techniques [64]. This observation of very large local deformation was in fact one of the reasons for developing a colloid model for C-S-H. This analysis seems to suggest that shrinkage at low rh's is due to removal of interlayer water.

The new concept resulting from the colloid or particular nature of C-S-H is that at about 40% rh, the meniscus disappears and the interface enters the SGP. This point is analogous to the critical point in colloid science [49]. At the local level, the gel continues to shrink only a small amount or even expands as the attractive forces between globules are relaxed. This marks a transition from the influence of capillary stress to the influence of surface energy, which introduces a new mechanism associated with reversible shrinkage.

3.2.3. Comments on creep and temperature — aging

Changes in microstructure due to load are much less studied than changes due to drying. However, it seems likely that similar mechanisms apply to shrinkage and creep, except that deformation is now driven by shear stress and not compression. Creep is also greatly reduced at relative humidities less than 50% [65]. The experiments establishing this were performed by increasing the relative humidity on dried samples, interpreted here as meaning creep begins when SGP are full and increases as the LGP fill at higher rh's. Creep may involve reorientation of the globules producing tighter local packing and perhaps reducing the surface area. Both creep and shrinkage may involve changes in the LGP. Research into the microstructural changes that occur under load is an area that should produce dividends.

The collapse of LGP not only occurs with drying (and probably under load), but also with heat and slowly with the passage of time [11]. Under these latter conditions the stress is not large enough to cause bulk deformation. The LGP are part of the LD structure, which is the modification of C-S-H that is deforming. That the LGP can be reduced in volume (forming a different density LD C-S-H) without bulk deformation suggests that the as formed non-deforming HD C-S-H is percolated through the paste, and as long as the stress is not too high, HD resists deformation.

Reduction in the LGP with the passage of time bears a striking resemblance to the concept of aging as proposed by Bazant et al. [66] in that it is a microstructural change that is associated with the gradual removal of the mechanism of irreversible shrinkage and/or creep with the passage of time, and is not associated with the formation of new product. The gradual, over periods of years, reduction of the LGP is further evidenced by the observation [67] that the water content of the C-S-H gel, which according to CM-II includes the water in the LGP, is reduced with the passage of time. The H/S decreases with time from 4.46 at 3 days to 3.93 at 28 days to 3.6 at 60 days and finally to 3.2 between 126 and 479 days [47].

Aging and change in volume of the LGP appear to be correlated. The removal of LGP is almost certainly driven by an associated reduction in surface energy, a process that is accelerated by the application of capillary stress, applied stress, or heat. These effects could be coupled in a non-linear fashion.

As discussed, the globules deform as water is removed from and reenters the interlayer spaces. On rewetting, this water takes between 10 and 100 days to recover, similar to the reversible component of creep. Applied stress could also cause this deformation, and be associated with the reversible component of creep.

There are several ways of rearranging the particles to collapse the LGP and possibly different loading conditions lead to different results. Discrete particle mechanics should be able to solve at least some of these problems. Microstructural considerations should facilitate the modeling of the non-linear coupling of deformation due to applied stress plus changing moisture and/or temperature. The process of pulling water out of the LGP causes them to collapse, but the greatest collapse occurs while the meniscus is outside the gel, not in the LGP.

Interesting evidence for deformation of C-S-H comes from nitrogen surface area experiments, which show variation with

drying technique prior to measurement, harsher drying resulting in lower values. The values have a positive correlation [68] with the volume of pores in the 2–8 nm diameter range. These are the smallest pores accessible to nitrogen but are part of the LGP population. Also the value of the measured surface area is higher when samples are ground before drying compared with drying a small slab of material [27]. Grinding eliminates much of the capillary porosity and this removes the mechanism that collapses the LGP. On the other hand, if stress is applied and if capillary forces are maintained by drying, the net effect could amplify the deformation.

3.3. Hindered and constrained water — and disjoining pressure

Powers and Brownyard [30] described the origins of disjoining pressure in detail. They argued that surfaces attract water to reduce surface energy, and that this attraction would extend over several layers of water. When two close surfaces are separated by water- filled space but are not at their equilibrium separation, described recently by molecular models [69], then they are either attracted or repelled. In either case the water is under pressure different from that for bulk water, and can cause swelling or shrinkage.

Two other descriptions of water, based on theory and observation, have been introduced into the literature, namely "hindered water," and "constrained water." Hindered water was proposed as part of a theoretical construct to explain viscous flow [70,71], in and out of load bearing spaces with well-defined diffusion constants. Hindered water is to some extent load bearing and can slowly diffuse to accommodate deformation under load or during drying. This water diffuses very slowly and, according to CM-II, would require the globules to rearrange. In general, this coupling between redistribution of water and rearrangement of globules may account for the very long times required to reach equilibrium at any given relative humidity.

The constrained water, measured by QENS, is, in the CM-II model, quantitatively associated with the SGP, as described above. Indeed the reduction of LGP may be directly linked with the rearrangement of SGP, its quantity matching the space available in these small pores. Constrained water has thermodynamic characteristics between those of chemically bound water and liquid water. Some of the complex behavior regarding the removal and return of water to the smallest pores may well be related to the thermodynamics of constrained water. It would be very productive to further characterize constrained water to see if it can be related to the mechanisms of creep and shrinkage.

3.4. LD and HD C-S-H

C-S-H in cement paste forms as either LD, during the early stages of reaction (the first day or so), or later as HD, namely during the middle and late stage [1]. The amount of each type depends on variables such as initial water/cement. HD is more loosely packed than LD C-S-H, which was described in CM-I as spherical globules in a close packed arrangement, e.g. with a packing efficiency of 0.74. There is little reason to change this, but if shapes of the globules are different in HD, it is important that any model keeps the elastic properties of the individual C-S-H globules constant. If HD is granular, then it may also tolerate heterogeneity, or the presence of the large 10 nm pores, while maintaining a constant mean modulus (this is a concept that requires further research). If the particles are not spherical they can still slide over each other, but much less easily than in the LD C-S-H. While most of this paper has addressed refinements in the LD structure, the HD structure is also important.

Water can penetrate all of the pores in C-S-H, both LD and HD. Inspection of published data [72] shows that the adsorption isotherm does not depend on variables such as water/cement ratio, up to about 40% rh. Noting that the centers of the fractal structures in the LD C-S-H are as densely packed as in the HD C-S-H, and that only the smallest pores are filled at 40% rh, one can conclude that the low-pressure portion of the isotherm should not depend on the amount of LD and HD.

Strength may develop as globule flocs interpenetrate (Fig. 5). The LGP are between the flocs and the SGP within the flocs. Aging is a process of interpenetration of globule flocs which reduces the volume of LGP. The interface between LGP and capillary pores may be thought of as the outer surface of C-S-H. In this region the globule flocs may be isolated and nearest neighbors may not interpenetrate. The size of the globule flocs is between 30–60 nm depending on drying and age, which is about the same size as features seen using microscopic techniques such as atomic force microscopes (see for example Ref. [18]).

3.5. Implications of CM-II to strength and toughness

Recently [73] arguments have been presented suggesting that HD C-S-H forms in restricted space and LD C-S-H forms in more open areas. This reflects the reason that the concept of HD and LD was chosen as opposed to "inner" and "outer" product, having as a boundary the original cement clinker surface, a concept not supported by observation. This model was used to determine the distribution of HD and LD.

CM-II provides a few hints about the influence of relative humidity on fracture strength and toughness. The strength of the LD may be related to the interpenetration of the globular flocs. As described above, the water–air interface is about to enter the SGP at 50% rh. Strikingly, the toughness of a paste peaks at this rh [74]. The meniscus applies a closing stress, which is at its maximum at 50% rh. In other words the bonds between grains are increased by the meniscus, which is exerting a compressive stress on the pores or a closing stress at the crack tip. Tensile (bending) strength does not appear to be influenced much by relative humidity [72]. Tensile strength of a brittle material depends on the flaw size and on the intrinsic strength of the matrix. Compressive strength appears to be increased on drying [75].

4. Summary

Several refinements have been made to CM-I. CM-II is a model of the nanostructure of C-S-H that builds on CM-I. Starting with precise values for the water content and physical density of a globule, the model defines distinct pore and interlayer spaces that

allow quantitative interpretation of literature data for density and water content of C-S-H at different relative humidities. The C-S-H is treated as an assembly of globules which are not spherical, with a cross section of 5 nm. The globules are particles of nanometer dimension that assemble into statistically well-defined patterns. Water-filled spaces include the interlayer spaces, the intraglobule spaces (IGP), the small gel pores (SGP), and the large gel pores (LGP), in each of which the water has a specific thermodynamic character.

The strong hysteresis in the low-pressure portion of the water isotherm is interpreted as representing water that leaves the interlayer spaces at pressures below 11% or so and not reentering until higher pressures. Research into the thermodynamics of the water in the smallest pores holds promise. The most tightly bound water is adsorbed on the surface of the globules and within the IGP.

Possible mechanisms for irreversible shrinkage and reversible creep, neither of which has been previously addressed in the literature, are discussed. Irreversible shrinkage is associated with changes in structure of the LGP, and its associated SGP. Reduction in surface energy is probably the driving force for natural aging; and the non-linear coupling of stress, heat and drying may all result from the acceleration of these changes in structure under the influence of stress and heat. It is proposed that the globules can deform slowly, and that this deformation is recoverable reversible.

The presumption of globules, or particles with an outer surface and internal porosity, as well as interlayer space, is used to model the density of C-S-H under various moisture conditions. The model reconciles various density values reported in the literature without requiring water to have an unlikely density that is far different from 1 Mg/m^3. While this does not preclude density variation near the surface and within the interlayer space, these variations would be much smaller than the 10% or more that is often cited in the literature.

Globules are particles that can rearrange under stress, which opens the door to modeling mechanical properties using granular mechanics, and holds particular promise for understanding viscous flow and the irreversible deformation of concrete. This model predicts that one consequence of the irreversible changes that occur because of drying, heating, and the passage of time is a measurable decrease in the LGP, that is pores between about 3–12 nm in diameter. The SGP may also rearrange, with changes in associated constrained water.

Acknowledgment

Special thanks to Jeff Thomas for comments and ideas. This research was supported by NSF grant # CMS-0409571.

References

[1] H.M. Jennings, A model for the microstructure of calcium silicate hydrate in cement paste, Cem. Concr. Res. 30 (2000) 101–116.
[2] H.M. Jennings, Reply to the discussion of the paper "A model for the microstructure of calcium silicate hydrate in cement paste" by Ivan Odler, Cem. Concr. Res. 30 (8) (2000) 1339–1341.
[3] H.M. Jennings, Colloid model of C-S-H and implications to the problem of creep and shrinkage, Mat. Struct./Concr. Sci. Eng. 37 (2004) 59–70.
[4] J.J. Thomas, H.M. Jennings, A colloidal interpretation of chemical aging of the C-S-H gel and its effects on the properties of cement paste, Cem. Concr. Res. (2006) 30–38.
[5] C.M. Neubauer, H.M. Jennings, The use of digital images to determine deformation throughout a microstructure, part II: application to cement paste, J. Mater. Sci. 35 (22) (2000) 5751–5765.
[6] G.W. Scherer, Structure and properties of gels, Cem. Concr. Res. 29 (1999) 1149–1157.
[7] J.J. Thomas, H.M. Jennings, A colloidal interpretation of chemical aging of the C-S-H gel and its effects on the properties of cement paste, Cem. Concr. Res. (2006) 30–38.
[8] G. Constantinides, F. Ulm, K. Van Vliet, On the use of nanoindentation for cementitious materials, Mat. Struct. 36 (257) (2003) 191–196.
[9] G. Constantinides, F.-J. Ulm, The effect of two types of C-S-H on the elasticity of cement-based materials: results from nanoindentation and micromechanical modeling, Cem. Concr. Res. 34 (1) (2004) 67–80.
[10] G. Constantinides, F.J. Ulm, The nanogranular nature of C-S-H, J. Mech. Phys. Solids 55 (2007) 64–90.
[11] H.M. Jennings, J.J. Thomas, J.S. Gevrenov, G. Constantinides, F.-J. Ulm, A multi-technique investigation of the nanoporosity of cement paste, Cem. Concr. Res. 37 (2007) 329–336.
[12] E. Robens, B. Benzler, G. Buchel, H. Reichert, K. Schumacher, Investigation of characterizing methods for the microstructure of cement, Cem. Concr. Res. 32 (1) (2002) 87–90.
[13] A.J. Allen, R.C. Oberthur, D. Pearson, P. Schofield, C.R. Wilding, Development of the fine porosity and gel structure of hydrating cement systems, Philos. Mag., B 56 (3) (1987) 263–268.
[14] J.J. Thomas, H.M. Jennings, A.J. Allen, The surface area of cement paste as measured by neutron scattering — evidence for two C-S-H morphologies, Cem. Concr. Res. 28 (6) (1998) 897–905.
[15] A.J. Allen, J.J. Thomas, H.M. Jennings, Composition and density of nanoscale calcium–silicate–hydrate in cement, Nat. Mater. 6 (4) (2007) 311–316.
[16] J.J. Thomas, J.J. Chen, H.M. Jennings, Effects of decalcification on the microstructure and surface area of cement paste, Cem. Concr. Res. 34 (2003) 2297–2307.
[17] S. Garrault, E. Finot, E. Lesniewska, A. Nonat, Study of C-S-H growth on C3S surface during its early hydration, Mat. Struct. 38 (278) (2005) 435–442.
[18] A. Nonat, The structure and stoichiometry of C-S-H, Cem. Concr. Res. 34 (2004) 1521–1528.
[19] I.G. Richardson, The nature of C-S-H in hardened cements, Cem. Concr. Res. 29 (1999) 1131–1147.
[20] H.F.W. Taylor, Cement Chemistry, 2nd ed.Thomas Telford, London, 1997.
[21] R.F. Feldman, P.J. Sereda, A model for hydrated Portland cement paste as deduced from sorption-length change and mechanical properties, Mat. Struct. 1 (6) (1968) 509–520.
[22] M. Daimon, S.A. Abo-El-Enein, G. Hosaka, S. Goto, R. Kondo, Pore structure of calcium silicate hydrate in hydrated tricalcium silicate, J. Am. Ceram. Soc. 60 (3–4) (1977) 110–114.
[23] R.F. Feldman, Changes to structure of hydrated Portland cement on drying and rewetting observed by helium flow techniques, Cem. Concr. Res. 4 (1974) 1–11.
[24] V.S. Ramachandran, R.F. Feldman, J.J. Beaudoin, Concrete Science, Heyden, London, 1981.
[25] S. Brunauer, S.A. Greenberg, The hydration of tricalcium silicate and β-dicalcium silicate at room temperature, Proceedings of the Fourth International Symposium on the Chemistry of Cements, National Bureau of Standards, Washington, D.C., 1960.
[26] S. Brunauer, P.H. Emmit, E. Teller, Adsorption of gases in multimolecular layers, J. Am. Chem. Soc. 60 (1938) 309–319.
[27] C.M. Hunt, Nitrogen sorption measurements and surface areas of hardened cement pastes, Symposium on Structure of Portland Cement Paste and Concrete, Special Report, vol. 90, Highway Research Boad, Washington, D.C., 1966, pp. 113–122.
[28] E.E. Bodor, J. Skalny, S. Brunauer, J. Hagymassy, M. Yudenfreund, Pore structures of hydrated calcium silicates and Portland cements by nitrogen adsorption, J. Colloid Interface Sci. 34 (4) (1970) 560–570.
[29] R.S. Mikhail, S.A. Selim, Adsorption of organic vapors in relation to pore structure of hardened Portland cement paste, Symposium of Structure of

Portland Cement and Concrete, Highway Research Board Special Report, vol. 90, 1966, pp. 123–134.
[30] T.C. Powers and T.L. Brownyard, Studies of the Physical Properties of Hardened Portland Cement Paste. Journal of the American Concrete Institute, 1947. 43: p. 101–132, 249–336, 469–504, 549–602, 669–712, 845–57, 865–880, 933–969, 971–992; reprinted in PCA Bull. 22 Portland Cement Association, 1948, 992 pp.
[31] S. Brunauer, A discussion of the helium flow results of R. H. Feldman, Cem. Concr. Res. 2 (4) (1972) 489–492.
[32] R.F. Feldman, Helium flow characteristics of rewetted specimens of dried hydrated Portland cement paste, Cem. Concr. Res. 3 (1973) 777–790.
[33] R. Rarick, J. Bhatty, H.M. Jennings, Surface area measurement using gas sorption: applications to cement paste, in: J. Skalny, S. Mindess (Eds.), Materials Science of Concrete IV, The American Ceramic Society, Westerville, OH, 1995, pp. 1–39.
[34] R.F. Feldman, The flow of helium into the interlayer spaces of hydrated Portland cement paste, Cem. Concr. Res. 1 (1971) 285–300.
[35] R.F. Feldman, Reply to discussion by S. Brunauer, Cem. Concr. Res. 2 (4) (1972) 493–498.
[36] S. Brunauer, Further discussion of the helium flow results of R. F. Feldman, Cem. Concr. Res. 2 (1972) 749–753.
[37] R.F. Feldman, Reply to Brunauer's second discussion of "helium flow measurements", Cem. Concr. Res. 2 (1972) 755.
[38] T.C. Powers, The thermodynamics of volume change and creep, Mater. Constr. 1 (6) (1968) 487–507.
[39] T.C. Powers, Structure and physical properties of hardened Portland cement paste, J. Am. Ceram. Soc. 41 (1958) 1–6.
[40] R.F. Feldman, P.J. Sereda, A model for hydrated Portland cement paste as deduced from sorption-length change and mechanical properties, Mat. Struct. 1 (6) (1968) 509–520.
[41] J.F. Young, W. Hansen, Volume relationships for C-S-H formation based on hydration stoichiometries, Materials Research Society Symposium Proceedings, Materials Research Society, Boston, 1987, pp. 313–321.
[42] P.D. Tennis, H.M. Jennings, A model for two types of calcium silicate hydrate in the microstructure of Portland cement pastes, Cem. Concr. Res. 30 (6) (2000) 855–863.
[43] A.L. Pulin, A.A. Fomkin, V.A. Sinitsyn, A.A. Pribylov, Adsorption and adsorption-induced deformation of NaX zeolite under high pressures of carbon dioxide, Russ. Chem. Bull. Int. Ed. 50 (1) (2001) 60–62.
[44] J. Adolphs, Excess surface work — a modeless way of getting surface energies and specific surface areas directly from sorption isotherms, Appl. Surf. Sci. 253 (2007) 5645–5649.
[45] J.M. Cases, I. Berend, M. Francois, P.J. Uriot, L.J. Michot, F. Thomas, Mechanism of adsorption and desorption of water vapor by homoionic montmorillonite: 3. the Mg^{2+}, Ca^{2+}, Sr^{2+} and Ba^{2+} exchanged forms, Clays Clay Miner. 45 (1) (1997) 8–22.
[46] R.F. Feldman, Mechanism of creep of hydrated Portland cement paste, Cem. Concr. Res. 2 (1972) 521–540.
[47] H.J.H. Brouwers, The work of Powers and Brownyard revisited: part I, Cem. Concr. Res. 34 (2004) 1697–1716.
[48] H. Roper, Dimensional change and water sorption studies of cement paste, Symposium on Structure of Portland Cement Paste and Concrete, 1966, pp. 74–83, Special report 90, Washington, D.C.
[49] C.J. Brinker, G.W. Scherer, Sol–Gel Science, Academic Press, New York, 1990, p. 908.
[50] J.J. Thomas, S.A. FitzGerald, D.A. Neumann, R.A. Livingston, The state of water in hydrating tricalcium silicate and Portland cement pastes as measured by quasi-elastic neutron scattering, J. Am. Ceram. Soc. 84 (8) (2001) 1811–1816.
[51] J. Adolphs, Physico-mechanical and chemical properties of hardened cement paste interacting with moisture, 2nd International RILEM Symposium of Advances in Concrete through Science and Engineering, RILEM Publications SARL, Essen, Germany, 2006, pp. 181–193.
[52] A. Donev, I. Cisse, D. Sachs, E.A. Variano, F.H. Stillinger, R. Connelly, S. Torquato, P.M. Chaikin, Improving the density of jammed disordered packings using ellipsoids, Science 303 (2004) 990–993.
[53] H.M. Jennings, Reply to the discussion of the paper "A model for the microstructure of calcium silicate hydrate in cement paste" by Ivan Odler, Cem. Concr. Res. 30 (8) (2000) 1339–1341.
[54] R.S. Mikhail, S.A. Abo-El-Enein, Studies on water and nitrogen adsorption on hardened cement pastes I development of surface in low porosity pastes, Cem. Concr. Res. 2 (1972) 401–414.
[55] J.J. Thomas, A.J. Allen, J.J. Chen, H.M. Jennings, Structural Changes to the Calcium Silicate Hydrate Gel Phase of Hydrated Cement on Drying and Resaturation, in preparation.
[56] M. Oda, Initial fabrics and their relationships to mechanical properties of granular material, Soil Found. 12 (1) (1972) 17–36.
[57] L.J. Parrott, J.F. Young, Effect of prolonged drying on the silicate structure of hydrated alite pastes, Cem. Concr. Res. 11 (1981) 11–17.
[58] R.F. Feldman, Mechanism of creep of hydrated Portland cement paste, Cem. Concr. Res. 2 (1972) 521–540.
[59] S. Mindess, J.F. Young, D. Darwin, Concrete, 2nd ed., Prentice Hall, Englewood Cliffs, NJ, 1996, p. 644.
[60] J.K. Mackenzie, The elastic constants of a solid containing spherical holes, Proc. Phys. Soc. B 63 (1950) 2–11.
[61] O. Coussy, P. Dangla, T. Lassabatere, V. Baroghel-Bouny, The equivalent pore pressure and the swelling and shrinkage of cement-based materials, Mat. Struc. 37 (265) (2004) 15–20.
[62] G. Constantinides, F.-J. Ulm, The effect of two types of C-S-H on the elasticity of cement-based materials: results from nanoindentation and micromechanical modeling, Cem. Concr. Res. 34 (1) (2004) 67–80.
[63] M.J. Setzer, The solid–liquid gel system of hardened cement paste, 2nd International RILEM Symposium on Advances in Concrete through Science and Engineering, RILEM Publications SARL, Essen, Germany, 2006, p.
[64] C.M. Neubauer, T.B. Bergstrom, K. Sujata, Y. Xi, E.J. Garboczi, H.M. Jennings, Drying shrinkage of cement paste as measured in an environmental scanning electron microscope and comparison with microstructural models, J. Mater. Sci. 32 (1997) 6415–6427.
[65] F. Wittmann, Einfluss des Feuchtigkeitsgehaltes auf das Kriechen des Zementsteines, Rheol. Acta 9 (1970) 282–287.
[66] Z.P. Bazant, A.B. Hauggaard, S. Baweja, F.J. Ulm, Microprestress solidification theory for concrete creep. I: aging and drying effects, J. Eng. Mech., ASCE 123 (1997) 1188–1194.
[67] P. Lu, G. Sun, J.F. Young, Phase composition of hydrated DSP cement pastes, J. Am. Ceram. Soc. 76 (4) (1993) 1003–1007.
[68] M.C. Garci Juenger, H.M. Jennings, The use of nitrogen adsorption to assess the microstructure of cement paste, Cem. Concr. Res. 31 (6) (2001) 883–892.
[69] A. Gmira, M. Zabat, R.J.M. Pellenq, H. Van Damme, Microscopic physical basis of the macroscopic poromechanical behavior of concrete, Mat. Struc. 37 (275) (2004) 3–13.
[70] Z.P. Bazant, Thermodynamics of hindered absorption and its implications for hardened cement paste and concrete, Cem. Concr. Res. 2 (1972) 1–16.
[71] F. Beltzung, F.H. Wittmann, Role of disjoining pressure in cement based materials, Cem. Concr. Res. 35 (12) (2005) 2364–2370.
[72] P.J. Sereda, R.F. Feldman, E.G. Swenson, Effect of sorbed water on some mechanical properties of hydrated Portland cement pastes and compacts, Symposium on Structure of Portland Cement Paste and Concrete, Highway Research Board, Washington, D.C., 1966, pp. 58–73.
[73] V. Smilauer, Z. Bittnar, Microstructure-based micromechanical prediction of elastic properties in hydrating cement paste, Cem. Concr. Res. 36 (2006) 1708–1718.
[74] J.J. Beaudoin, Meniscus effects and fracture in Portland cement paste, J. Mater. Sci. Lett. 5 (1986) 1107–1108.
[75] G.G. Garrett, H.M. Jennings, R.B. Tait, The fatigue hardening behaviour of cement-based materials, J. Mater. Sci. 14 (1979) 296–306.
[76] V.S. Ramachandran, Differential thermal method of estimating calcium hydroxide in calcium silicate and cement pastes, Cem. Concr. Res. 9 (1979) 677–684.